A 2E Analysis and Optimization of a Hybrid Solar Humidification-Dehumidification Water Desalination System and Solar Water Heater

Bazregari, Mohammad Javad
Faculty of Mechanical and Energy Engineering, Shahid Beheshti University, Tehran, I.R. IRAN

Norouzi, Nima
Department of Energy Engineering and Physics, Amirkabir University of Technology (Tehran Polytechnic), Tehran, I.R. IRAN

Gholinejad, Mahdi
Faculty of Mechanical and Energy Engineering, Shahid Beheshti University, Tehran, I.R. IRAN

Fani, Maryam*[+]
Department of Energy Engineering and Physics, Amirkabir University of Technology (Tehran Polytechnic), Tehran, I.R. IRAN

ABSTRACT: *This study presents an energy-exergy analysis of a Humidification-Dehumidification (HD) solar water desalination system. The extensive application of the HD system lies in its low energy consumption and ability to exploit solar energy to supply all the heat energy demands. The unsteady governing equations were solved until the system reached a steady state. The simulations were done with the Euler approach to solving the system of energy balance equations numerically. This study's main goal was to investigate the effect of different configurations of the hybrid system and various operating conditions on the performance of the solar HD water desalination system. The optimum configuration was selected based on thermodynamic and exergy analyses. The effects of important parameters such as inlet water and air mass flow rate in the humidifier and dehumidifier water temperature and mass flow rate on the system's operation were studied. This paper also explored the feasibility of the extra heat as a domestic water heater under various conditions. Based on exergy analysis, it is shown that the solar desalination system with air-water preheater with the power of 1057.9 W had the most exergy destruction in comparison with the two other systems (i.e., water preheater system and air preheater system with the respective exergy destructions of 901.3 W and 75.3 W). Comparing the values of freshwater production, exergy destruction, and exergy efficiency, the solar system with a water preheater was selected as the optimum one.*

KEYWORDS: *Solar water desalination; HD desalination; Energy-exergy analysis; Solar desalination system.*

***** *To whom correspondence should be addressed.*
+ E-mail: mfani@aut.ac.ir
1021-9986/2022/6/2135-2152 18/$/6.08

INTRODUCTION

Nowadays, drought and the increase in population have resulted in a freshwater shortage for some people, mostly living in arid areas. Approximately 1 out of 6 people in the world are dealing with the problem of freshwater availability. About 70% of the people in the world will face a lack of drinking water by 2025, while almost 50% of them live in places less than 200 km distance from the sea. Interestingly, 70% of the earth's surface is covered with water; but, just 3% of this water is freshwater, and most of this amount is stored as ice in Greenland and Poles. Therefore, almost 1% of the water in the world should supply human beings' demand for freshwater [1]. Considering these issues, alongside the fact that there is a huge amount of brine water in the oceans and seas and local sources of brine water in deserts, researchers and desalination industries have been motivated to study and optimize different methods of water purification [2]. Most of these methods have high energy consumption and usually use the waste heat of power plants. Furthermore, water desalination plants suffer from pollution due to the usage of fossil fuels and contamination due to chemical materials used for pre-purification. Thus, there is no significant development in the technological and commercial aspects of small thermal water desalination systems.

Asbik et al. [3] presented an exergy analysis for a solar water desalination system coupled with a thermal energy storage system utilizing phase change materials. *Diaf et al.* [4] investigated solar desalination from an economical point of view. Their method contained several solar distillation stages for the small-scale production of freshwater. *Chafidz et al.* [5] presented a portable and integrated solar desalination system that operates based on membrane distillation for arid remote areas in Saudi Arabia. This system can be used in areas with no electricity and drinking water. It can be also applied in emergency conditions such as natural disasters. *Qtaishat* and *Banat* [6] presented a small-scale low-temperature solar desalination system based on membrane distillation. *Rodriguez et al.* [7] applied low-pressure vapor in the solar collector for water desalination, however, the main problems were the size and cost of this system.

Other studies have shown that the cost of freshwater production with common methods such as MSF (Multi-Stage Flash), ME (Multi-Effect), and VC (Vapor Compression) at rates lower than 100 m^3/day will significantly increase by the decline of the production capacity limiting the application of these methods for small scale water desalination [8]. The current paper will study the Humidification-Dehumidification (HD) desalination approach due to increasing attention focused on this method in recent years. Low energy consumption and the ability to use solar energy to supply the total thermal energy demand are among the special features of this method.

HD desalination system includes a humidifier tower, storage tank, and dehumidifier heat exchanger. This method operates in three stages: first, warm air enters the humidifier tower. In this stage, brine water from the storage tank is added to the warm air to increase its moisture content. In the next stage, warm, humid air passes through the dehumidifier condenser coils; freshwater is produced upon condensation of the vapor. The outlet brine water returns to the storage tank to further humidify the warm air in the humidifier tower. Many researchers presented various thermodynamic analyses and optimization schemes for the HD desalination system [9-13].

Nawayseh et al. [14, 15] showed that HD solar desalination with the process is an effective approach to extract freshwater from brine. *Zhang et al.* [16] numerically investigated an HD desalination system integrated with a heat pump. Their results showed an enhancement in the system efficiency by increasing inlet brine water, humid air flow rate, and air temperature. They also computed the Gained Output Ratio (GOR) and the cost (per kg of freshwater production). *Ahmad et al.* [17] experimentally studied an HD desalination system containing wavy aluminum sheets in the humidifier to inspect the effect of parameters such as temperature and flow rate of the input brine water, water-to-air mass ratio, and the flow rate of cooling water entering the dehumidifier, on the system performance and efficiency. For example, they found that reducing the cooling water temperature from 28.5 to 17^{o}C will raise the production rate from 10 to 15 L/h. *He et al.* [18] studied an HD desalination system with low waste heat from a thermo-economical point of view. Their simulations were carried out with closed water and air cycle assumption. Besides the GOR and freshwater production rate, the maximum required investment was also calculated.

Farid et al. [19] offered a mathematical model to study the HD process. Their results clarified the effects of

various parts of the system on the performance and production rate. Their optimization method was, however, so complicated. *Hou et al.* [20, 21] presented a method to optimize the performance of an HD solar desalination system. The optimum water-to-dry air mass flow rate ratio was obtained with the aim of pinch figures.

Capocelli et al. [22] proposed an HD desalination system using multi-stage vapor absorption. Their proposed system had high energy consumption but unique features such as high flexibility and good recovery and GOR rate, which thermodynamically justified its utilization.

Nafey et al. [23] generated a mathematical model to investigate the effect of climate and operational conditions on the performance of solar HD systems. Their paper indicated that the system's performance is strongly related to the air and cooling water mass flow rate and the rate of received solar energy.

Orfi et al. [24] theoretically and experimentally studied a solar HD desalination system. To improve the system's performance, they used the latent heat of the condensed vapor to preheat the feed water.

Yamali et al. [25] theoretically investigated an HD solar desalination system with a double-pass flat plate solar air heater. The effect of different system operating conditions, types of air heaters, and some different design parameters and weather conditions on the performance of the mentioned system was considered under the climatological condition of Ankara. Their results showed that the system's productivity could increase up to 8% if a double-pass solar air heater is used instead of a single-pass solar air heater; moreover, about 30% reduction was observed without a double-pass solar air heater under the same operating condition.

A study by *Kariman* [26] on desalination systems is considered one of the promising solutions to deal with the water scarcity problem. The multi-effect type is getting more popular among different kinds of desalination systems, with advantages like using low-grade thermal resources. Considering the mentioned issues, in this study, a high-performance Multi-Effect Desalination (MED) system is introduced, and the enhancement potential is evaluated in detail. The introduced and reference designs are compared together from different points of view. The results showed that the freshwater production of the introduced MED device is enhanced from the range of 12-16 to 14-21.6 L/h compared to the base case condition, but also gained output ratio increases up to 30%-40%. Moreover, the conducted exergy analysis shows that with an exergy efficiency of 82%, the brine tank has the highest performance among other components, while the exergy destruction for this part is negligible compared to the other parts. Therefore, a high level of improvement can be achieved using the introduced design.

In a research by *Hosseinzadeh et al.*[27], the integrated carbon dioxide power cycle with the geothermal energy source to supply the required reverse osmosis desalination power for freshwater production is defined. The cycling power is consumed by the desalination system and sodium hypochlorite generator. Exergoeconomic analysis and optimization are studied. Exergoeconomic analysis shows that the desalination system, sodium hypochlorite generator, carbon dioxide turbine, and natural gas turbine have the highest rate of capital gain and exergy destruction cost. For the first case of optimization, the total cost rate is considered the objective function. The optimal inlet discharge rate of the sodium hypochlorite generator was 62% of the desalination system's brine water outlet discharge rate. Plus, the total cost rate is reduced by 10% compared to the general case when 100% of the brine water discharge rate of the desalination system enters into the sodium hypochlorite generator. The second case is multiobjective optimization to reduce costs and increase productivity.

In research by *Kariman et al.* [28], energy analysis is first carried out to identify the major energy-consuming equipment and the electrical energy consumed in the system. The exergy analysis of the system showed that the most exergy destruction occurs in the boiler compartment and central heat exchanger. The system is designed for a tank capacity of approximately 11.3m^3, so the freshwater output is 9.6 m^3, and we reported freshwater production in every process. This process takes about 4.5 h. So the system's capacity is about 2200 lit/hour. Finally, the system was optimized to reduce energy consumption and increase freshwater production using a two-objective genetic algorithm. Optimization results showed that 59.83 L of fresh water per kWh was generated.

In research by *Kariman et al.* [29], different desalination systems and their governing equations are studied. Then the energy consumption of an evaporative vacuum easy desalination system with a brine tank is modeled. This modeling and the equations governing

the energy consumption of new subsets such as the evaporator, condenser, vacuum pump, and other pumps are presented. In the end, the economic modeling of the system is investigated. The system's feasibility is reported in three cities (Abu Dhabi, Las Palmas, and Perth). The results show that the pumps' annual operating cost is estimated to be 0.19 M€/yr, 0.51 M€/yr, and 0.14 M€/yr for Abu Dhabi and Las Palmas, and Perth, respectively. Also, the annual cost of freshwater production is compared with other reaches in these cities. The results are shown that Perth has the lowest cost of freshwater output at 0.67 M€/yr, and Las Palmas has the highest cost of freshwater production at 0.104 M€/yr. The reason is the difference in the electricity prices in these cities.

Another research by *Yargoli et al.* [30] defines the integrated carbon dioxide power cycle with a geothermal energy source to supply the required reverse osmosis desalination power for freshwater production. It is also a carbon dioxide power cycle, coupled with thermal energy recovery of infrared energy of Liquid Natural Gas (LNG) to generate more power. A sodium hypochlorite generator is considered to prevent the brine water from discharging. The brine water portion of the desalination outlet was the input to this generator. The cycling power is consumed by the desalination system and sodium hypochlorite generator. After modeling, the advanced exergy analyses are studied. By exergy analysis, it is observed that in this model, the condenser has the highest exergy destruction rate, equal to 952 kW. Additionally, the unavoidable part of the exergy destruction of carbon dioxide turbines constitutes 88% of its exergy destruction, equal to 301 kW. So this component is the best option to improve exergy destruction.

Previous works have addressed the thermodynamic analysis of the solar HD desalination system and the effect of various factors on the efficiency and performance of the system. But, to the best of the authors' knowledge, there is no research exploring the influence of different configurations of inlet water and air heating on the system's performance. Therefore, the present paper is aimed to conduct an energy-exergy analysis to select the best configuration. The effect of various operating conditions such as temperature and mass flow rate of inlet water and air on freshwater production will also be discussed. The other novelty of this paper lies in the feasibility of using the dehumidifier outlet water waste heat for supplying domestic hot water.

THEORETICAL SECTION

This section provides the equations required for modeling three different configurations of the HD system. The classification is based on preheating inlet water and air to study their effect on the production rate. The first case is the solar desalination system with the air preheater, the second is the solar desalination system with the water preheater, and the last one is the system with both air and water preheater[31-34].

HD system with air preheater and flat collector

In this system, ambient air is preheated after entering the upper channel of the solar collector. Preheated air gets warmer in the lower channel of the collector. It then enters the humidifier, and the remaining stages are the same as the previously mentioned stages for the HD system. This configuration is schematically depicted in Fig. 1 [35].

HD system with water preheater and parabolic collector

In this configuration, air enters the humidifier without preheating, but the brine water is preheated in the parabolic collector before entering the storage tank. The other stages are the same as the previously described systems. A schematic view of this configuration is shown in Fig. 2 [36].

HD system with air and water preheater

This system combines the two previous systems in which both water and air are preheated before entering the HD system. The schematics of this configuration are illustrated in Fig. 3 [37].

EXPERIMENTAL SECTION

Assumption

For energy equilibration of each system element, the following assumptions were used as heat losses from the collector edges, water storage tank, humidifier, and dehumidifier to the environment are neglected. In both solar passages, radiation energy absorbed by the airflow will be neglected. There is no leakage during air passage through the solar collector, humidifier tower, and dehumidifier heat exchanger. Air temperature difference changes linearly in the streamwise direction. The fully

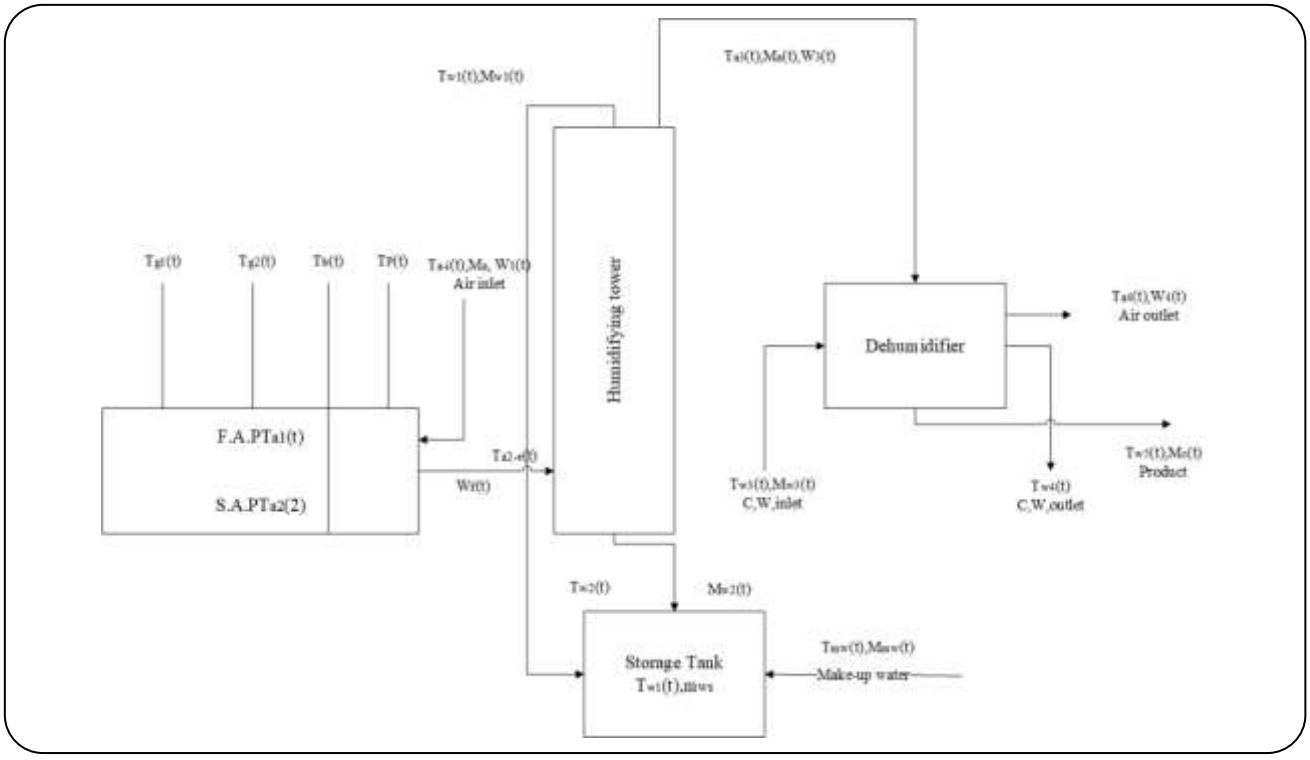

Fig. 1: Schematics of the HD desalination with air preheater.

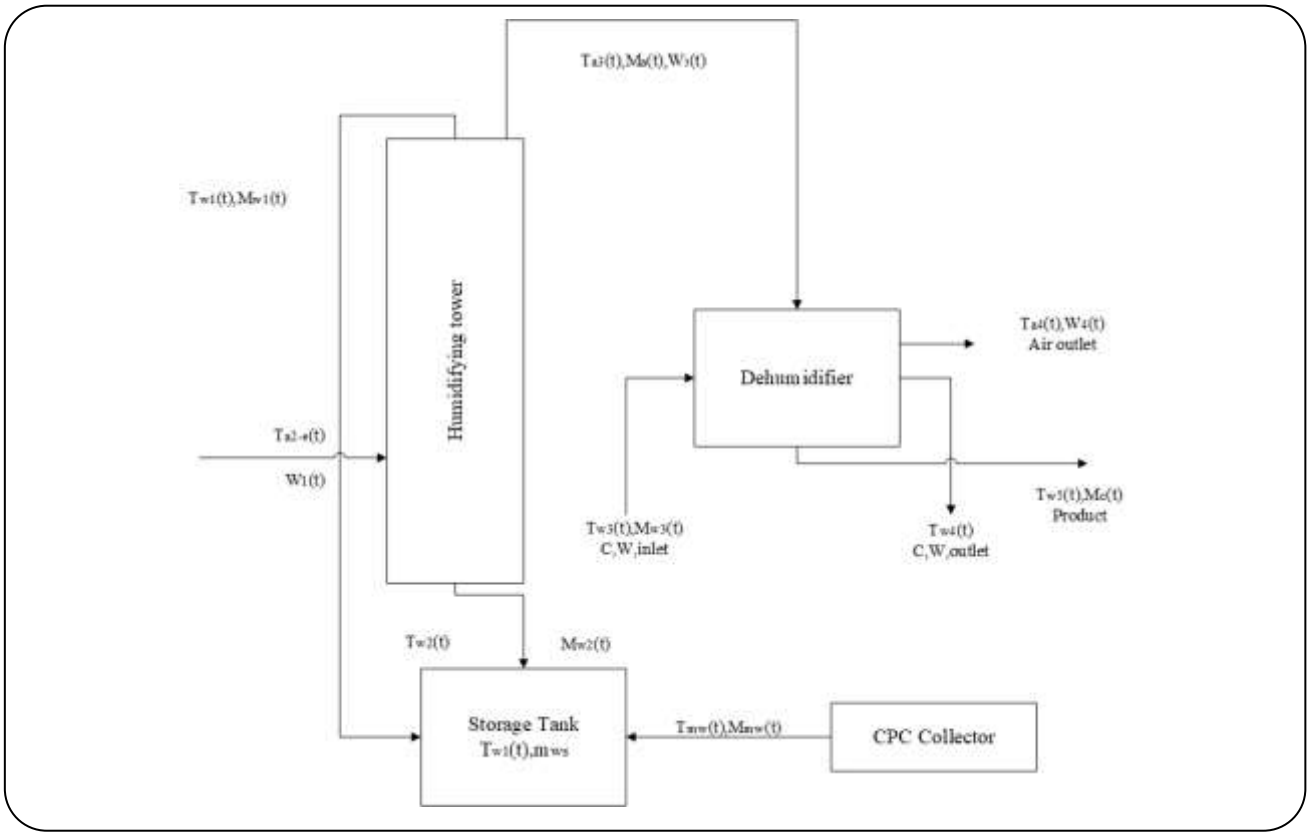

Fig. 2: Schematics of HD system with water preheater.

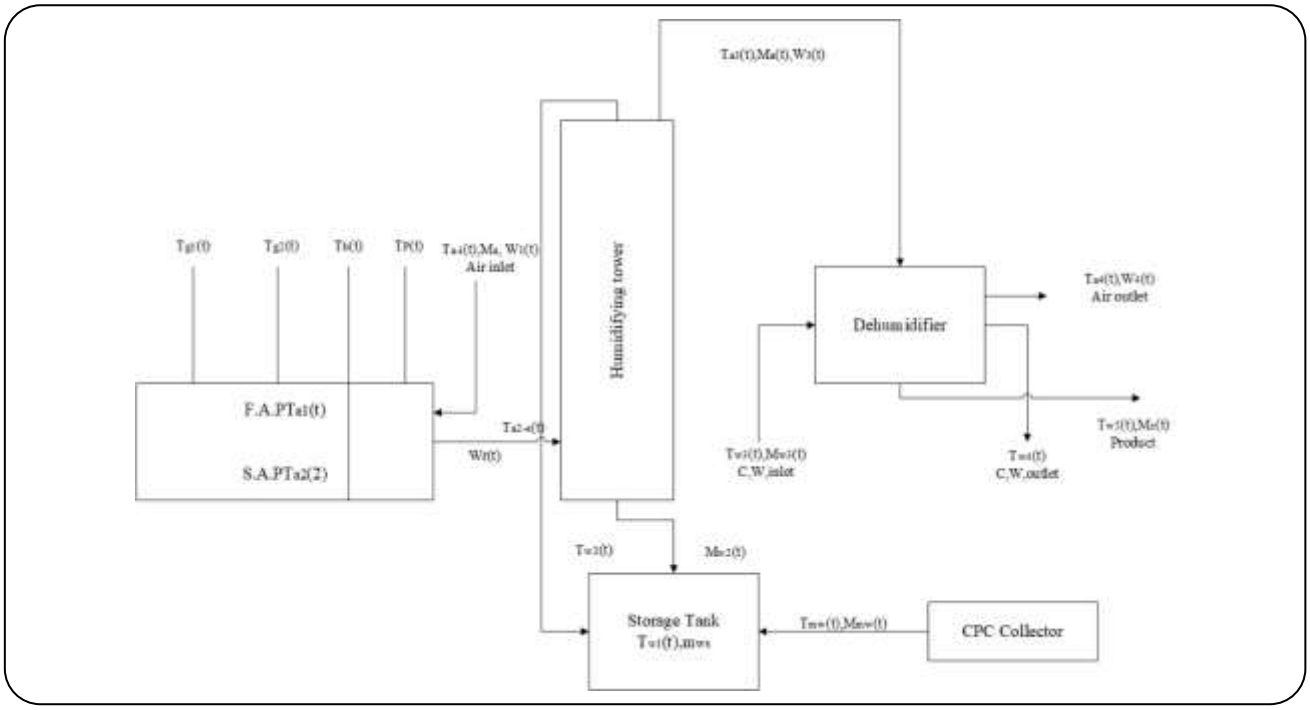

Fig. 3: The schematics of the HD desalination system with air and water preheating.

developed laminar or turbulent flow is considered. The outlet water temperature is equal to the outlet air wet-bulb temperature of the dehumidifier. Dehumidification is done on a saturation curve. Condensed water and outlet cooling water temperatures are equal to the dehumidifier's outlet air dry-bulb temperature. The temperature gradient in the water storage tank is neglected. The Humidifier inlet water temperature is the same as the storage tank water temperature. Cooling water temperature is assumed to be constant throughout the day. Ambient temperature, wind speed, and relative humidity are set as their value at 12 pm. The solar radiation is 700 at 12 pm.

Energy balance equations

Energy balance equations for air heaters are as follows [25-28]:

Second glass cover:

$$m_g.C_{p-g}.\frac{dT_{g2}}{dt} = I.\alpha_g.A_c + q_{r,g1-g2} - q_{c,g2-amb} - q_{r,g2-sky} + q_{c,g1-g2} \quad (1)$$

First glass cover:

$$m_g.C_{p-g}.\frac{dT_{g1}}{dt} = I.\alpha_g.\tau_g.A_c - q_{r,g1-g2} - q_{c,g1-a1} + q_{r,p-g1} - q_{c,g1-g2} \quad (1)$$

First air pass:

$$m_a.C_{p-a}.\frac{dT_{a1}}{dt} = q_{c,p-a1} + q_{c,g1-a1} - M_aC_{p-a}(T_{a1-e} - T_{a-i}) \quad (3)$$

Absorber plate:

$$m_p.C_{p-p}.\frac{dT_p}{dt} = I.\alpha_p.\tau_g^2.A_c - q_{c,p-a2} - q_{c,p-a1} - q_{r,p-g1} - q_{r,p-b} \quad (4)$$

Second air pass:

$$m_a.C_{p-a}.\frac{dT_{a2}}{dt} = q_{c,p-a2} + q_{c,b-a2} - M_aC_{p-a}(T_{a2-e} - T_{a1-e}) \quad (5)$$

Base plate:

$$m_b.C_{p-b}.\frac{dT_b}{dt} = q_{r,p-b} - q_{c,b-a2} - q_{1,b-amb} \quad (6)$$

Energy balance equations for the storage tank, humidifier, and dehumidifier are:

Water storage tank[36]:

$$m_{w1}.C_{p-w}.\frac{dT_{w1}}{dt} = M_{w2}(t).C_{p-w}.T_{w2}(t) + M_{mw}(t).C_{p-w}.T_{mw} - M_{w1}.C_{p-w}.T_{w1}(t) - q_{1,w1-amb} \quad (7)$$

Humidifier:

$$M_a.\left(h_{a3}(t)-h_{a2-e}(t)\right)=M_{w1}.C_{p-w}.T_{w1}(t)-M_{w2}(t).C_{p-w}.T_{w2}(t) \quad (8)$$

Dehumidifier:

$$M_a.\left(h_{a3}(t)-h_{a4}(t)\right)=M_{w3}.C_{p-w}.\left(T_{w4}(t)-T_{w3}\right)+M_c(t).C_{p-w}.T_{w5}(t) \quad (9)$$

Heat transfer terms in flat collector:

Heat transfer terms in the above Equations (1-9) are[37]:

$$q_{r,g1-g2}=A_c.h_{r,g1-g2}.\left(T_{g1}-T_{g2}\right) \quad (10)$$

$$A_c=w.L \quad (11)$$

The radiation heat transfer coefficient between two glass covers is:

$$h_{r,g1-g2}=\frac{\sigma.\left(T_{g1}^2+T_{g2}^2\right).\left(T_{g1}+T_{g2}\right)}{\left(\frac{1}{\varepsilon_{g1}}+\frac{1}{\varepsilon_{g2}}-1\right)} \quad (12)$$

$$q_{c,g2-amb}=A_c.h_{c,g2-amb}.\left(T_{g2}-T_{amb}\right) \quad (13)$$

The Convective heat transfer coefficient for the airflow above the glass cover can be obtained through empirical equations [38]:

$$h_{c,g2-amb}=2.8+3\,.V_{wind} \quad (14)$$

$$q_{r,g2-sky}=A_c.h_{r,g2-sky}.\left(T_{g2}-T_{sky}\right) \quad (15)$$

$$T_{sky}=T_{amb}-6 \quad (16)$$

The radiation heat transfer coefficient between the second glass cover and sky can be calculated as[39]:

$$h_{r,g2-sky}=\varepsilon_{g2}.\sigma.\left(T_{g2}^2+T_{sky}^2\right).\left(T_{g2}+T_{sky}\right) \quad (17)$$

$$q_{c,g1-g2}=A_c.h_{c,g1-g2}.\left(T_{g1}-T_{g2}\right) \quad (18)$$

The natural convection heat transfer coefficient between the first and second glass covers has the following form[40]:

$$h_{c,g1-g2}=Nu_{g1-g2}.\frac{K_a}{x} \quad (19)$$

To calculate the Nusselt number, the following relation is proposed [25]:

$$Nu_{g1-g2}=1+1.44\times\left[1-\frac{1708}{Ra\times CosB}\right]^{+} \times\left(1-\frac{(Sin1.8\times B)^{1.6}\times 1708}{Ra\times CosB}\right)+\left[\left(\frac{Ra\times CosB}{5830}\right)^{1/3}-1\right]^{+} \quad (20)$$

In the above equation, $+$ exponent means that for negative values, those terms will be zero. Also, Ra is defined as[41]:

$$Ra=\frac{g.\beta.\left(T_{g1}-T_{g2}\right).x^3}{\alpha\times\upsilon} \quad (21)$$

Thermal properties of humid air can be proposed as a function of air temperature [42]:

$$K=0.024+0.6773\times10^{-4}\times T \quad (22)$$

$$\alpha=7.7255\times10^{-10}\times T^{1.83} \quad (23)$$

$$\upsilon=0.1284\times10^{-4}+0.00105\times10^{-4}\times T \quad (24)$$

$$q_{c,g1-a1}=A_c.h_{c,g1-a1}.\left(T_{g1}-T_{a1}\right) \quad (25)$$

The forced convection heat transfer coefficient inside the upper channel of double pass flat plate solar air heater can be expressed as[43]:

$$h_{c,g1-a1}=Nu_{g1-a1}.\frac{K_a}{D_h} \quad (26)$$

$$D_h=\frac{4.\ A_{sec}}{(2\ .\ w+2\ .D)} \quad (27)$$

$$Nu_{g1-a1}=4.9+\frac{0.0606.\ (Re_{a1}.Pr.D_h/L)^{1.2}}{1+0.0909.(Re_{a1}.Pr.D_h/L)^{0.7}.Pr^{0.17}} \quad (28)$$

$$Nu_{g1-a1}=\frac{(f_{a1}/8)\times(Re_{a1}-1000)\times Pr}{1+12.7\times(f_{a1}/8)^{0.5}\times(Pr^{0.67}-1)} \quad (29)$$

$$Re_{a1}=\frac{V_{a1}+D_h}{V_{a1}} \quad (30)$$

$$f_{a1}=(0.79\times\ln Re_{a1}-1.64)^{-2} \quad (31)$$

$$q_{r,p-g1}=A_c.h_{r,p-g1}.\left(T_p-T_{g1}\right) \quad (32)$$

The radiation heat transfer coefficient between the copper absorption plate and the glass cover can be determined by[44]:

$$h_{r,g1-g2}=\frac{\sigma.\left(T_{g1}^2+T_p^2\right).\left(T_{g1}+T_p\right)}{\left(\frac{1}{\varepsilon_{g1}}+\frac{1}{\varepsilon_p}-1\right)} \quad (33)$$

$$q_{c,p-a1}=A_c.h_{c,p-a1}.\left(T_p-T_{a1}\right) \quad (34)$$

$$h_{c,p-a1}=h_{c,g1-a1} \quad (35)$$

Considering assumption 4, $T_{a1_e}$is defined as:

$$T_{a1_e}=2\,.T_{a1}-T_{a_i} \quad (36)$$

$$q_{c,p-a2} = A_c.h_{c,p-a2}.(T_p - T_{a2}) \quad (37)$$

For calculating $h_{c,p-a2}$, the relation for $h_{c,g1-a1}$ can be useful, in which in all T_{a1}: terms are replaced by T_{a2_e}

$$h_{c,b-a2} = h_{c,p-a2} \quad (38)$$

$$q_{c,b-a2} = A_c.h_{c,b-a2}.(T_b - T_{a2}) \quad (39)$$

$$q_{r,p-b} = A_c.h_{r,p-b}.(T_p - T_b) \quad (40)$$

$$h_{r,p-b} = \frac{\sigma.(T_p^2 + T_b^2).(T_p + T_b)}{\left(\frac{1}{\varepsilon_p} + \frac{1}{\varepsilon_b} - 1\right)} \quad (41)$$

$$q_{1,b-amb} = A_c.U_{loss}.(T_b - T_{amb}) \quad (42)$$

$$M_{w2}(t) = M_{w1} - M_a.(W_3(t) - W_1(t)) \quad (43)$$

$$T_{w2}(t) = T_{a3}(t) \quad (44)$$

$$M_c(t) = M_a.[W_3(t) - W_4(t)] \quad (45)$$

$$T_{a4}(t) = T_{w4}(t) = T_{w5}(t) \quad (46)$$

$$M_{mw}(t) = M_a.[W_3(t) - W_1(t)] \quad (47)$$

$$q_{1,w1-amb} = A_c.U_{loss}.(T_{w1} - T_{amb}) \quad (48)$$

Heat transfer terms in parabolic collector

The part of solar energy absorbed by the fluid in the pipe is called useful energy and the fluid in the absorber pipe is called Heat Transfer Fluid (HTF). Thus, useful energy can be calculated as [45]:

$$Q_u = F_R[I\,A_{ap} - A_r U_L(T_i - T_{ap})] \quad (49)$$

$$A_{ap} = (W - D_g) \times L \quad (50)$$

$$A_r = \pi D_o L \quad (51)$$

Absorbed energy by HTF results in a temperature rise:

$$Q_u = Mc_p(T_o - T_i) \quad (52)$$

$$F_R = \frac{Mc_p}{A_r U_L}\left[1 - \exp\left(-\frac{U_L F' A_r}{Mc_p}\right)\right] \quad (53)$$

$$F' = \frac{\frac{1}{U_L}}{\frac{1}{U_L} + \frac{D_o}{h_{fi} D_i} + [\frac{D_o}{2k} \ln \frac{D_o}{D_i}]} \quad (54)$$

$$Nu = \frac{h_{fi} D_i}{k_f} \quad (55)$$

Nusselt number for laminar flow is assumed to be 4.364 and for turbulent flow following equations can be used[46]:

$$Nu = 0.023(Re)^{0.8}(Pr)^{0.4} \quad (56)$$

$$Re = \frac{\rho V D_i}{\mu} \quad (57)$$

$$Pr = \frac{c_p \mu}{k_f} \quad (58)$$

$$U_L = [\frac{1}{h_r} + \frac{1}{h_c}]^{-1} \quad (59)$$

$$h_w = \frac{(Nu)k_w}{D_g} \quad (60)$$

$$Nu = 0.4 + 0.54(Re)^{0.52}, \qquad 0.1 < Re < 1000 \quad (61)$$

$$Nu = 0.3(Re)^{0.6}, \qquad 1000 < Re < 50{,}000 \quad (62)$$

$$h_r = \varepsilon_r \sigma(T_r + T_{ap})(T_r^2 + T_{ap}^2) \quad (63)$$

Exergy equations

$$ex_K = \frac{1}{2} m v^2 \quad (64)$$

$$ex_P = mgh \quad (65)$$

$$ex_{ph} = (h - h_0) - T_0(s - s_0) \quad (66)$$

$$ex_{ch} = \sum_{i=1}^{N} y_i e_{xi}^{ch} + RT_0\left(\sum_{i=1}^{N} y_i \ln(y_i)\right) \quad (67)$$

$$ex_w = W \quad (68)$$

$$Ex_q = Q\left(1 - \frac{T_0}{T}\right) \quad (69)$$

$$ex = ex_K + ex_P + ex_{ph} + ex_{ch} \quad (70)$$

$$Ex_D = Ex_{in} - Ex_{out} + Q_i \times \left(1 - \frac{T_0}{T_i}\right) - W \quad (71)$$

$$\eta = \frac{\sum \text{Exergy out}}{\sum \text{Exergy in}} = 1 - \frac{Ex_D}{\sum Ex_{in}} \quad (72)$$

Solution procedure and validation

A computer code was developed based on the above energy and exergy balance equations to investigate the effect of different configurations for inlet air and preheated water to select the best case. Using this code, the influence of various parameters on the HD desalination system can be studied. This code simultaneously and unsteadily solves the energy balance equations using the Euler method. The Timestep was ½, and the initial values of T_{g1}, T_{g2}, T_{a1}, T_{a2}, and T_{w1} were set as ambient temperature while T_b and T_p

Table 1: Basic design parameters and operating conditions of the desalination system.

Parameter	Value	Parameter	Value
Solar air heater width (m)	0.5	glass Specific heat (J/kg°C)	800
Solar air heater length (m)	1.0	Basin plate Specific heat (J/kg°C)	385
Channel thickness (m)	0.05	Absorption plate Specific heat (J/kg°C)	385
Distance between two glass covers(m)	0.025	Air Specific heat (J/kg°C)	1006
Mass glass(kg)	3.75	Water Specific heat (J/kg°C)	4178
Mass Basin plate(kg)	4.50	Solar air heater area (m^2)	1.0
Mass Absorption plate(kg)	4.50	Loss heat transfer coefficient (W/m^2K)	0.75
First glass cover Emissivity	0.90	Second glass cover Emissivity	0.90
Base plate cover Emissivity	0.95	Absorption plate cover Emissivity	0.95
Glass Absorptivity	0.05	Absorption plate Absorptivity	0.95
Glass Transmissivity	0.95	Solar collector slope	0.05
Stored water mass (kg)	500	Storage tank water Mass flow rate (kg/s)	0.028
Air Mass flow rate (kg/s)	0.027	Humidifier inlet water mass flow rate (kg/s)	0.05
Make-up water Temperature (℃)	20	Humidifier inlet water Temperature (℃)	20
Ambiental Temperature (℃)	25	Wind velocity(m/s)	5

were 5 and 10 ℃ above the ambient temperature, respectively. These temperatures were used for determining temperature-dependent heat transfer coefficients. Using these initial temperatures and calculating heat transfer coefficients, the above system of first-order ordinary differential equations was numerically solved to obtain the final temperatures. Thus, for a given humidifier inlet water and air temperatures at each time step, the outlet air temperature of the humidifier and dehumidifier can be calculated by equations 8 and 9, respectively. In the dehumidifier, condensed water in each time step can be calculated using equation 45 by knowing inlet and outlet air temperatures. The humidity and enthalpy of saturated air can be estimated using empirical relations as a function of air temperature:

$$W = 7.7e^{-7} \times T^3 - 1.95e^{-5} \times T^2 + 0.00071 \times T + 0.002 \quad (73)$$

$$h_a = 2.85e^{-5} \times T^4 - 0.00106 \times T^3 + 0.0615 \times T^2 + 1.32 \times T + 10.5 \quad (74)$$

The basic design parameters and operating conditions used in the solar desalination system are listed in Table 1.

To validate the simulation results of the proposed HD solar desalination system, the results of [25] were used. Fig. 4 shows the variation of freshwater production rate during a day versus inlet water mass flow rate for three different air mass flow rates. As can be seen, productivity increases with the mass flow rate of water and air, which is consistent with the findings of [25]. The differences between the results can be due to the lack of information presented in [25], such as the HD desalination system, environmental conditions, e.g., solar radiation intensity, the surrounding temperature, wind velocity, air relative humidity, and chemical features of saline water.

RESULTS AND DISCUSSION

In this section, first, different configurations (Figs. 1-3) for air and water preheating were to select the best one. Then, the effect of important parameters, such as humidifier inlet water and mass flow rates and dehumidifier inlet water temperature and mass flow rate, on freshwater production rate and dehumidifier outlet water temperature (to use for building heating) was investigated. Furthermore,

domestic hot water demand for a building with 4 residents was calculated and compared with the model results.

Comparing and choosing the best preheating configuration

Fig. 5 illustrates the effect of humidifier inlet water mass flow rate on freshwater production for three studied cases. As can be seen, the production rate for the system with air preheating was lower than the two other systems (which are almost the same). Fig. 6 also presents the effect of the humidifier inlet water mass flow rate on the dehumidifier outlet water temperature for three different configurations. Accordingly, there is no significant temperature difference in outlet heat water between the cases.

According to Figs. 5 and 6, it can be concluded that water preheating is better than air preheating for the HD desalination system due to its higher freshwater productivity and higher temperature provided for the desalination system in a similar capacity. To select the best case, the extra cost due to the air heating flat plate collector should be added, and thus, according to the insignificant effect of flat plate solar collector, only water preheating was selected.

Parametric study of the selected configuration

Figs. 7 and 8 depict the variation of produced freshwater with time and water temperature for the case with water preheating, respectively. It can be seen that the amount of freshwater production increased over time as a result of the temperature rise of humidifier inlet water due to solar energy absorption. After about 50 seconds, about 0.015 kg of fresh water was produced. Based on Fig. 8, after about 5 seconds, the outlet water temperature from the dehumidifier reached approximately a constant value (72.5 ^{o}C). Thus, water preheating only affects freshwater production and does not change the outlet water temperature.

Figs. 9 and 10 illustrate the dependence of the freshwater production rate on humidifier inlet water mass flow rate and dehumidifier inlet water mass flow rate, respectively. An increase in both parameters enhanced productivity. Indeed, when the inlet water mass flow rate increases, the humidity of the air got intensifies, and by the rise of the cooling system inlet water mass flow rate, the higher amount of moisture in the air will be condensed thus, the produced water mass flow rate will further enhance.

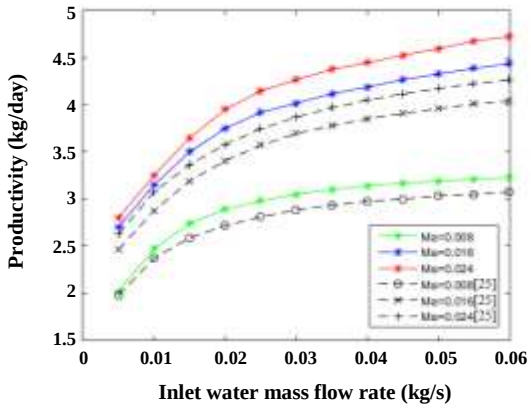

Fig. 4: The productivity rate versus inlet water mass flow rate for three different air mass flow rates compared with [25].

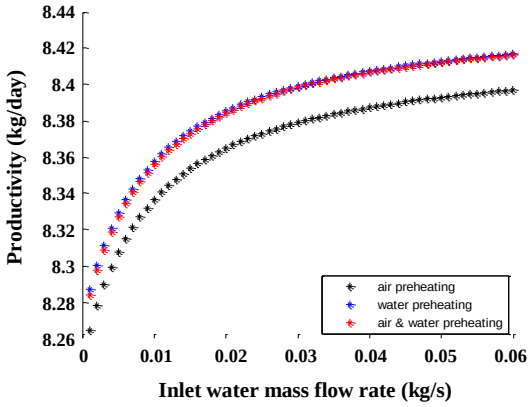

Fig. 5: The freshwater production rate versus inlet water mass flow rate for three studied configurations.

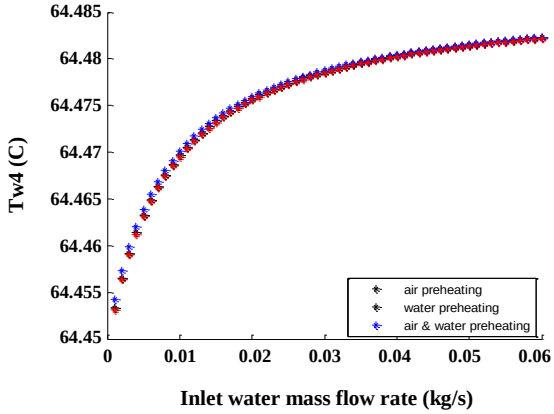

Fig. 6: Outlet cooling water temperature (Tw4) versus inlet water mass flow rate for three studied configurations.

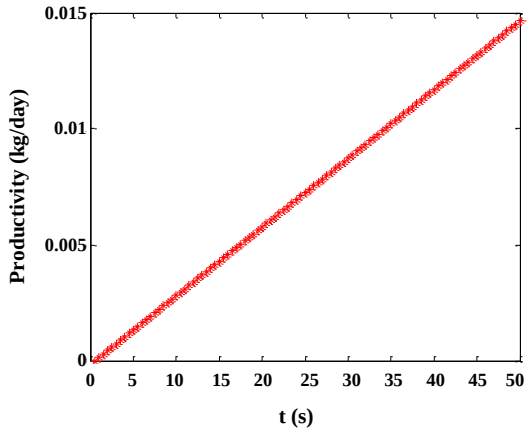

Fig. 7: Freshwater productivity rate in water preheating case.

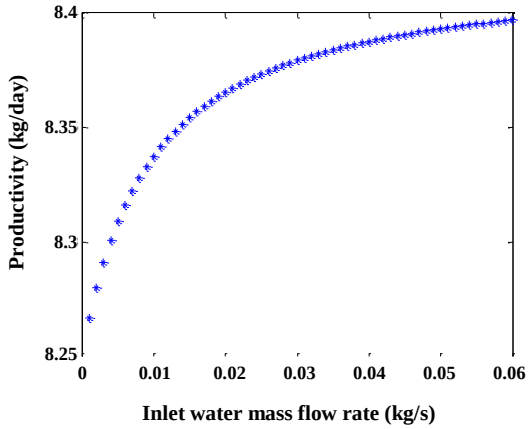

Fig. 9: Productivity variation with humidifier inlet water mass flow rate in the configuration with water preheating.

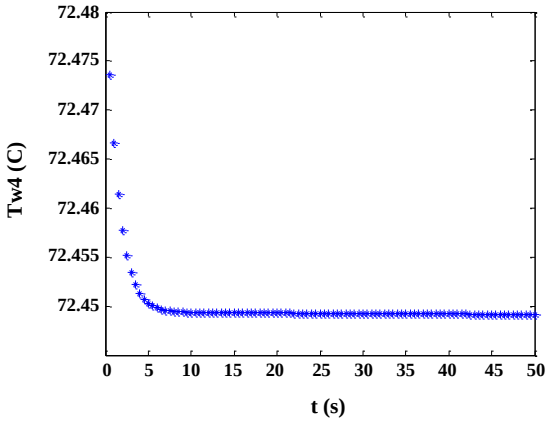

Fig. 8: Variation of Outlet cooling water temperature with time in water preheating case.

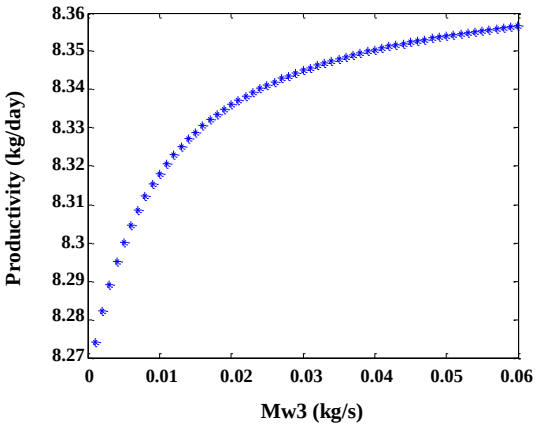

Fig. 10: Productivity versus dehumidifier inlet water mass flow rate in the configuration with water preheating.

Fig. 11 shows that the humidifier inlet water mass flow rate has a higher impact on the productivity rate than the dehumidifier inlet water mass flow rate. According to Fig. 12, the humidifier inlet water mass flow rate had a negligible effect on the dehumidifier outlet water temperature. The effect of the dehumidifier inlet water mass flow rate on the temperature of dehumidifier outlet water is also shown in Fig. 13. Due to the constant value of heat transfer, the outlet water temperature from this device is reduced by the elevation of the dehumidifier inlet water mass flow rate.

Fig. 14 shows the variation of dehumidifier inlet water temperature influence on the freshwater production rate. As can be observed, this parameter has a negligible effect on the production rate.

As discussed before and shown in Fig. 15, the production rate dramatically increased with the humidifier inlet air mass flow rate. The change in inlet air mass flow rate from 0.008 to 0.024 Kg/s augmented the temperature of water used for building heating from 61.2 to 64.4^{o}C. This can be assigned to the rise of production with the air mass flow rate (Fig. 4), which enhanced the heat transfer rate in the heat exchanger. Therefore, its temperature grew at a constant value of cooling water mass flow rate.

The effect of radiation on the temperature of water utilized for heating is depicted in Fig. 16. Based on the results, the radiation intensity had no significant impact on the dehumidifier outlet water temperature used for building heating. Because as radiation intensity increased, the value of vaporization and humidity absorption also

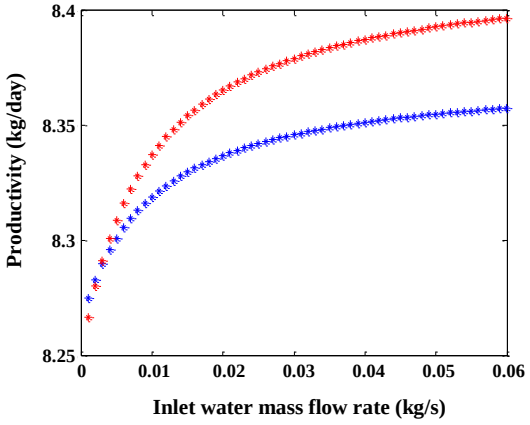

Fig. 11: The sensitivity of system productivity on M_{w1} and M_{w2} in the water preheating case.

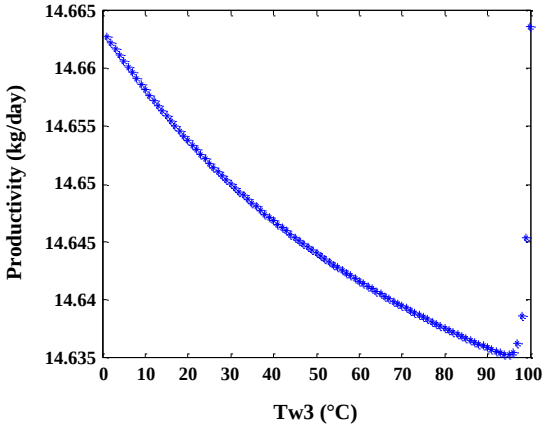

Fig. 14: Freshwater productivity rate versus Tw3 in water preheating case.

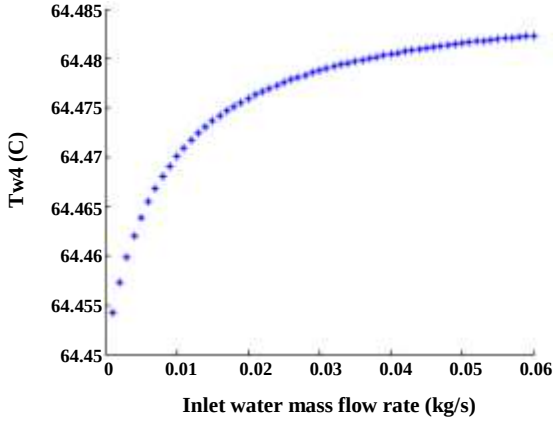

Fig. 12: T_{w4} variation with humidifier inlet water mass flow rate in the water preheating case.

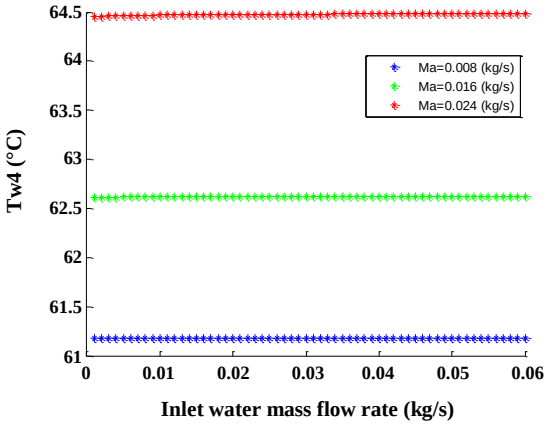

Fig. 15: Tw4 variation versus humidifier inlet water mass flow rate in different values of system inlet air mass flow rate in water preheating case.

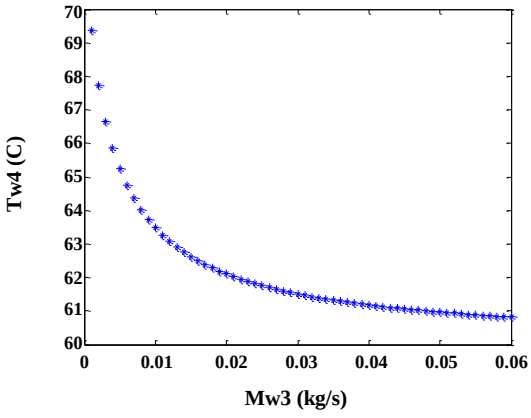

Fig. 13: T_{w4} variation with dehumidifier inlet water mass flow rate in the water preheating case.

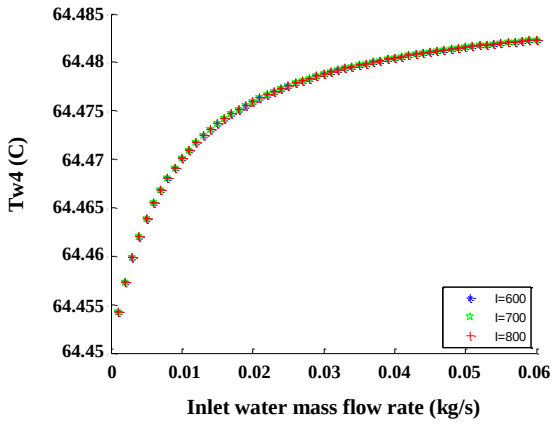

Fig. 16: Tw4 variations with humidifier inlet water mass flow rate in different solar radiation rate for water preheating case.

enhanced in the humidification system. Thus, the production rate increased at a constant mass flow rate and temperature of cooling water.

In addition to freshwater production, the HD solar system with water preheating also aims to supply hot water for a building. The maximum hot water demand of a building with four residents was easily calculated as about 0.0252 kg/s. As shown in Fig. 17, the hot water temperature dramatically decreased with the rise in consumption. Therefore, providing total domestic hot water demand, the water temperature experienced a reduction. Thus, a secondary solar collector is required to compensate for this reduction in the outlet water from the system. It is suggested that the mass flow of the consumption stay fixed in the optimum value and number of the heaters be increased where it is needed.

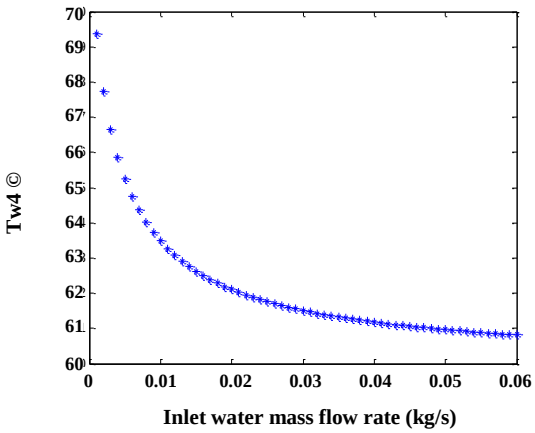

Fig. 17: Tw4 variations with Mw3 in water preheating case.

Exergy analysis of the system

Fig. 18 shows the effect of humidifier inlet water temperature on the humidification exergy efficiency for the three studied configurations. It can be easily concluded that exergy efficiency increased with the inlet water temperature of the humidifier. This behavior could be due to the higher vapor absorption ability at higher temperatures. Moreover, exergy efficiency in the air preheating case was lower than in the other cases.

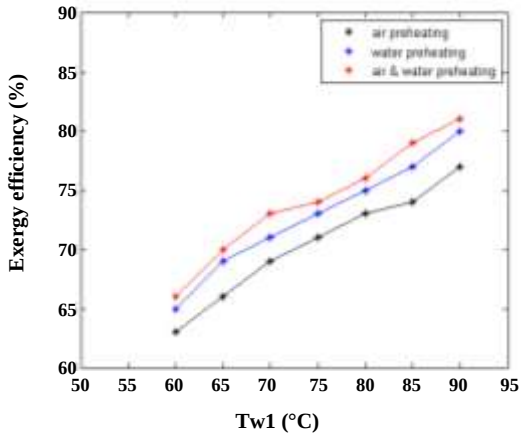

Fig. 18: Humidifier exergy efficiency variations with Tw1 for three different configurations.

Fig. 19 shows the impact of the cooling water temperature on the dehumidification exergy efficiency. As can be observed, the exergy efficiency showed an ascending trend with cooling water temperature. This behavior negatively affected the production rate. Thus, the optimum value of inlet cooling, water temperature should be determined through optimization methods. Another point is that the highest exergy efficiency was for both water and air preheating configurations.

The effect of humidifier inlet water temperature on storage tank exergy efficiency is illustrated in Fig. 20, which suggests a remarkable increase in exergy efficiency with the temperature. Again, the air-preheating configuration exhibited the lowest exergy efficiency (its maximum value is about 65% compared to 81% and 82.5% for water-preheating and air-water preheating configurations, respectively).

Fig. 21 presets the exergy destruction for different parts of the HD solar desalination system in the aforementioned configurations. The highest total exergy destruction

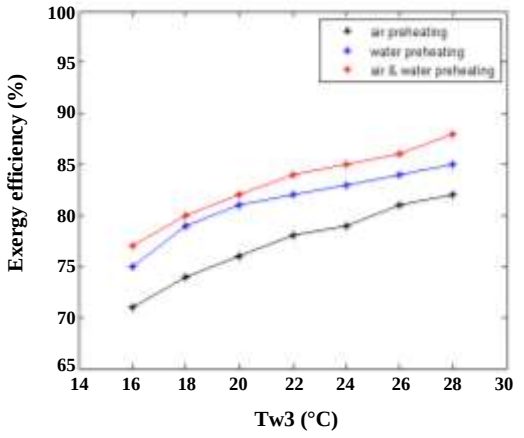

Fig. 19: Dehumidifier exergy efficiency variations with Tw3 for three different configurations.

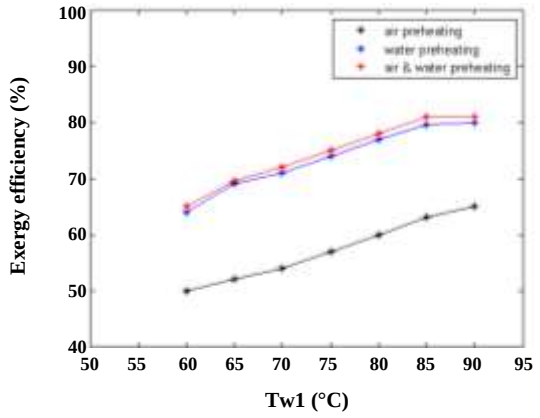

Fig. 20: Exergy efficiency variations for the storage tank with Tw1 for three different configurations.

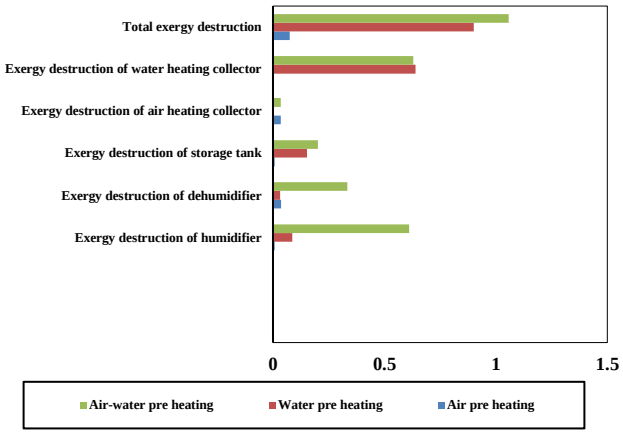

Fig. 21: Exergy destruction in different parts of the desalination system for three studied configurations.

was observed in the system with air-water preheating. For the air preheating configuration, the most exergy destruction was for the dehumidifier, while for the water preheating case, the most destruction was detected in the collector. The collector and humidifier exhibited the highest exergy destruction for the air-water preheating case.

According to the thermodynamic analysis, the best configuration for freshwater production was the one with water preheating. Based on exergy analysis, the water-preheating case had lower exergy destruction than the air-water preheating case. Thus, the energy and exergy analyses lead to selecting the water preheating configuration for the HD solar desalination system.

CONCLUSIONS

The present research uses energy-exergy equations to develop a code to model a solar HD desalination system. Three different configurations of desalination inlet air and water preheating were compared in terms of freshwater production rate and domestic hot water temperature. It is shown that HD solar desalination with water preheaters can result in the highest freshwater production. Moreover, the effect of various parameters such as humidifier and dehumidifier inlet water and air mass flow rates and the radiation value on the system performance was also explored. The system productivity was improved with the increase of humidifier inlet air and water mass flow rate and the temperature of dehumidifier inlet water.

The other factor studied in this paper was the cooling water mass flow rate, whose increase caused an enhancement in freshwater production but negatively impacted outlet heat water. As the dehumidifier inlet water mass flow rate is equal to this device's outlet water mass flow rate, this hot water can be used for a building with four residents. The heat water demand for such a building was estimated at 0.0252 kg/s, but the consumed heat water temperature decreased to supply the total demand, which can be compensated by utilizing a secondary collector. Comparing three different configurations with the aid of exergy analysis, the best choice was the water preheating case, whose exergy destruction was lower than the case with air-water preheating. Although air preheating configuration has the lowest exergy destruction, its production rate was also the lowest. Thus water preheating was selected as the best configuration for HD solar desalination system.

Nomenclature

A_c	Solar air heater area, m^2
A_{sec}	Solar air heater cross-section area, m^2
A_{ap}	Projected area of the parabolic collector, m^2
A_r	Lateral area of the parabolic collector, m^2
B	Solar collector slope
C_p	Specific heat, J/kg^oC
D	Channel thickness, m
D_h	Hydraulic diameter, m
F	Friction coefficient
g	Gravity
h	Enthalpy, J/kg
s	Entropy, J/kg^0C
h_c	Convective heat transfer coefficient, W/m^2K
h_r	Radiative heat transfer coefficient, W/m^2K

U_L	Total heat transfer coefficient, W/m^2K
I	Solar radiation, W/m^2
K	Conduction heat transfer coefficient, W/mK
W	Air moisture, kg_{water}/kg_{air}
w	Solar air heater width, m
x	Distance between two glass covers
ex_k	Kinetic exergy
ex_p	Potential exergy
ex_{ph}	Physical exergy
ex_{ch}	Chemical exergy
ex_w	Exergy of work
ex_q	Heat transfer exergy
ex_D	Exergy destruction
a	Ambient
a_i	Air
a1	Solar collector inlet air
a1_e	First air pass
a2	Outlet air from the upper channel of the collector
a2_e	Second air pass
a3	Collector outlet air
a4	Dehumidifier inlet air
w	Water
ap	Parabolic collector area
w1	Storage tank water
w2	Humidifier tower outlet water
L	Solar air heater length, m
M	Mass flow rate, kg/s
m	Mass, kg
M_{w1}	Humidifier inlet water mass flow rate, kg/s
Nu	Nusselt Number
Pr	Prandtl Number
q_c	Convection heat transfer rate, W
q_r	Radiation heat transfer rate, W
Ra	Rayleigh Number
Re	Reynolds Number
T	Temperature, ℃
t	Time, s
U_{loss}	Heat losses coefficient, W/m^2K
Q_u	Solar radiation absorbed by fluid inside the parabolic collector pipe, J
F_R	Heat extraction coefficient in parabolic collector
F'	Efficiency of the parabolic collector
V	Velocity, m/s
ex_D	Exergy destruction
ex_{in}	Inlet mass flow exergy
ex_{out}	Outlet mass flow exergy
η_{ex}	Exergy efficiency
α	Absorptivity
τ	Transmissivity
σ	Stefan-Boltzmann constant, W/m^2K^4
ε	Emissivity
β	Thermal expansion coefficient
υ	Kinematic viscosity
b	Basin plate
c	Condensed water
g	Glass cover
g1	First glass cover
g2	Second glass cover
1	Loss to ambient
mw	Make-up water
p	Absorption plate
w3	Cooling water entering dehumidifier
w4	Cooling water exiting dehumidifier
w5	Condensed water exiting dehumidifier

Received : Aug. 6, 2021 ; Accepted : Oct. 18, 2021

REFERENCES

[1] Mehanna M., Saito T., Yan J., Hickner M., Cao X., Huang X., Logan B.E., Using Microbial Desalination Cells to Reduce Water Salinity Prior to Reverse Osmosis, *Energy & Environmental Science*, **3(8)**: 1114-1120 (2010).

[2] Shannon M.A., Bohn P.W., Elimelech M., Georgiadis J.G., Marinas B.J., Mayes A.M., Science and Technology for Water Purification in the Coming Decades, *Nanoscience and Technology: A Collection of Reviews from Nature Journals*, 337-346 (2010).

[3] Asbik M., Ansari O., Bah A., Zari N., Mimet A., El-Ghetany H., Exergy Analysis of Solar Desalination Still Combined with Heat Storage System Using Phase Change Material (PCM), *Desalination*, **381**: 26-37 (2016).

[4] Diaf A., Cherfa A., Karadaniz L., Tigrine Z., A Technical–Economical Study of Solar Desalination, *Desalination*, **377**: 123-127 (2016).

[5] Chafidz A., Al-Zahrani S., Al-Otaibi M.N., Hoong C.F., Lai T.F., Prabu M., Portable and Integrated Solar-Driven Desalination System Using Membrane Distillation for Arid Remote Areas in Saudi Arabia, *Desalination*, **345**: 36-49 (2014).

[6] Qtaishat M.R., Banat F., Desalination by Solar Powered Membrane Distillation Systems, *Desalination*, **308**: 186-197 (2013).

[7] García-Rodríguez L., Palmero-Marrero A.I., Gómez-Camacho C., Application of Direct Steam Generation into a Solar Parabolic Trough Collector to Multieffect Distillation, *Desalination*, **125(1-3)**: 139-145 (1999).

[8] Soufari S.M., Zamen M., Amidpour M., Performance Optimization of the Humidification–Dehumidification Desalination Process Using Mathematical Programming, *Desalination*, **237(1-3)**: 305-317 (2009).

[9] Khalil A., El-Agouz S.A., El-Samadony Y.A., Abdo A., Solar Water Desalination Using an Air Bubble Column Humidifier, *Desalination*, **372**: 7-16 (2015).

[10] El-Agouz S.A., Abd El-Aziz G.B., Awad A.M., Solar Desalination System Using Spray Evaporation, *Energy*, **76**:276-283 (2014).

[11] Zou Q., Liu X., Economic Effects Analysis of Seawater Desalination in China with Input–Output Technology, *Desalination*, **380**:18-28 (2016).

[12] Yao M., Woo Y.C., Tijing L.D., Shim W.G., Choi J.S., Kim S.H., Shon H.K., Effect of Heat-Press Conditions on Electrospun Membranes for Desalination by Direct Contact Membrane Distillation, *Desalination*, **378**: 80-91 (2016).

[13] He W.F., Han D., Yue C., Pu W.H., A Parametric Study of a Humidification Dehumidification (HDH) Desalination System Using Low Grade Heat Sources, *Energy Conversion and Management*, **105**: 929-937 (2015).

[14] Nawayseh N.K., Farid M.M., Al-Hallaj S., Al-Timimi A.R., Solar Desalination Based on Humidification Process—I. Evaluating the Heat and Mass Transfer Coefficients, *Energy Conversion and Management*, **40(13)**:1423-1439 (1999).

[15] Nawayseh N.K., Farid M.M., Omar A.A., Sabirin A., Solar Desalination Based on Humidification Process—II. Computer Simulation, *Energy Conversion and Management*, **40(13)**: 1441-1461 (1999).

[16] Zhang Y., Zhang H., Zheng W., You S., Wang Y., Numerical Investigation of a Humidification-Dehumidification Desalination System Driven by Heat Pump, *Energy Conversion and Management*, **180**: 641-653 (2019).

[17] Ahmed H.A., Ismail I.M., Saleh W.F., Ahmed M. Experimental Investigation of Humidification-Dehumidification Desalination System with Corrugated Packing in the Humidifier, *Desalination*, **410**: 19-29 (2017).

[18] He W., Yang H., Wen T., Han D., Thermodynamic and Economic Investigation of a Humidification Dehumidification Desalination System Driven by Low Grade Waste Heat, *Energy Conversion and Management*, **183**: 848-858 (2019).

[19] Farid M.M., Parekh S., Selman J.R., Al-Hallaj S., Solar Desalination with a Humidification-Dehumidification Cycle: Mathematical Modeling of the Unit, *Desalination*, **151(2)**: 153-164 (2003).

[20] Hou S., Ye S., Zhang H., Performance Optimization of Solar Humidification–Dehumidification Desalination Process Using Pinch Technology, *Desalination*, **183(1-3)**: 143-149 (2005).

[21] Hou S., Zeng D., Ye S., Zhang H., Exergy Analysis of the Solar Multi-Effect Humidification–Dehumidification Desalination Process, *Desalination*, **203(1-3)**:403-409 (2007).

[22] Capocelli M., Balsamo M., Lancia A., Barba D., Process Analysis of a Novel Humidification-Dehumidification-Adsorption (HDHA) Desalination Method, *Desalination*, **429**:155-166 (2018).

[23] Nafey A.S., Fath H.E., El-Helaby S.O., Soliman A.M., Solar Desalination Using Humidification Dehumidification Processes. Part I. A Numerical Investigation, *Energy Conversion and Management*, **45(7-8)**: 1243-1261 (2004).

[24] Nafey A.S., Fath H.E., El-Helaby S.O., Soliman A., Solar Desalination Using Humidification–Dehumidification Processes. Part II. an Experimental Investigation, *Energy Conversion and Management*, **45(7-8)**: 1263-1277 (2004).

[25] Orfi J., Laplante M., Marmouch H., Galanis N., Benhamou B., Nasrallah S.B., Nguyen C.T., Experimental and Theoretical Study of a Humidification-Dehumidification Water Desalination System Using Solar Energy, *Desalination*, **168**: 151-159 (2004).

[26] Yamalı C., Solmuş İ. Theoretical Investigation of a Humidification-Dehumidification Desalination System Configured by a Double-Pass Flat Plate Solar Air Heater, *Desalination*, **205(1-3)**:163-177 (2007).

[27] Kariman H., Hoseinzadeh S., Heyns P.S., Sohani A. Modeling and Exergy Analysis of Domestic MED Desalination with Brine Tank, *Desalination and Water Treatment*, **197**: 1-13 (2020).

[28] Hoseinzadeh S., Yargholi R., Kariman H., Heyns P.S., Exergoeconomic Analysis and Optimization of Reverse Osmosis Desalination Integrated with Geothermal Energy, *Environmental Progress & Sustainable Energy*, **39(5)**: e13405 (2020).

[29] Kariman H., Hoseinzadeh S., Heyns P.S. Energetic and Exergetic Analysis of Evaporation Desalination System Integrated with Mechanical Vapor Recompression Circulation, *Case Studies in Thermal Engineering*, **16**: 100548 (2019).

[30] Kariman H., Hoseinzadeh S., Shirkhani A., Heyns P.S., Wannenburg J. Energy and Economic Analysis of Evaporative Vacuum Easy Desalination System with Brine Tank, *Journal of Thermal Analysis and Calorimetry*, **140(4)**: 1935-1944 (2020).

[31] Yargholi R., Kariman H., Hoseinzadeh S., Bidi M., Naseri A., Modeling and Advanced Exergy Analysis of Integrated Reverse Osmosis Desalination with Geothermal Energy, *Water Supply*, **20(3)**: 984-996 (2020).

[32] Duffie J.A., Beckman W.A., Blair N., Solar Engineering of Thermal Processes, Photovoltaics and Wind, John Wiley & Sons (2020).

[33] Duffie J.A., Beckman W.A. Solar Thermal Engineering Processes, A Wiley Interscience publication, New York, USA. (1980).

[34] Zamen M., Soufari S.M., Vahdat S.A., Amidpour M., Zeinali M.A.A., Izanloo H., Aghababaie H., Experimental Investigation of a Two-Stage Solar Humidification–Dehumidification Desalination Process, *Desalination*, **332(1)**:1-6 (2014).

[35] Norouzi N., Fani M., Talebi S., Exergetic Design And Analysis of a Nuclear SMR Reactor Tetrageneration (Combined Water, Heat, Power, and Chemicals) With Designed PCM Energy Storage and a CO_2 Gas Turbine Inner Cycle, *Nuclear Engineering and Technology*, **53(2)**: 677-687 (2021).

[36] Norouzi N., Fani M., Energy and Exergy Analysis and Selection of the Appropriate Operating Fluid for a Combined Power and Hydrogen Production System Using a Geothermal Fueled ORC and a PEM Electrolyzer, *Iranian Journal of Chemistry and Chemical Engineering (IJCCE)*, **41(5):** 1786-1803 (2022).

[37] Norouzi N., Talebi S., Exergy, Economical and Environmental Analysis of a Natural Gas Direct Chemical Looping Carbon Capture and Formic Acid-Based Hydrogen Storage System, *Iranian Journal of Chemistry and Chemical Engineering (IJCCE)*, **41(4)**: 1436-1457 (2022).

[38] Khajehpour H., Norouzi N., Bashash Jafarabadi Z., Valizadeh G., Hemmati M., Energy, Exergy, and Exergoeconomic (3E) Analysis of Gas Liquefaction and Gas Associated Liquids Recovery Co-Process Based on the Mixed Fluid Cascade Refrigeration Systems, *Iranian Journal of Chemistry and Chemical Engineering (IJCCE)*, **41(4)**: 1391-1410 (2022).

[39] Shakouri M., Ghadamian H., Mohammadpour Bagheri F., Feasibility Study of Integrating Multi Effect Desalination and Gas Turbine Systems for Lavan Island Oil Refinery, *Iranian Journal of Chemistry and Chemical Engineering (IJCCE)*, **31(3)**: 115-124 (2012).

[40] Khoshrou I., Jafari Nasr M., Bakhtari K., Exergy Analysis of the Optimized MSFD Type of Brackish Water Desalination Process, *Iranian Journal of Chemistry and Chemical Engineering (IJCCE)*, **36(6)**: 191-208 (2017).

[41] Rahman F., Nabi Bidhendi G., Sharifi F., Mehrdadi N., Eco-Friendly Innovation for Electrical Conductivity Reduction of Persian Gulf Sea water Using Highly Efficient Recyclable Sorbent, *Iranian Journal of Chemistry and Chemical Engineering (IJCCE)*, **41(4):** 1322-1334 (2022).

[42] Fattahi M., Karamoddin M., Peyvandi K., Varaminian F., Effects of Halide Anions on Water Desalination based on Crystallization Methods: Freezing and Tetrahydrofuran Hydrate Formation, *Iranian Journal of Chemistry and Chemical Engineering (IJCCE)*, **41(3):** 925-935 (2022).

[43] Ahmadi A., Noorpoor A., Kani A., Saraei A., Modeling and Economic Analysis of MED-TVC Desalination with Allam Power Plant Cycle in Kish Island, *Iranian Journal of Chemistry and Chemical Engineering (IJCCE)*, **40(6):** 1882-1892 (2021).

[44] Jain D., Modeling the System Performance of Multi-Tray Crop Drying Using an Inclined Multi-Pass Solar Air Heater with in-Built Thermal Storage, *Journal of Food Engineering*, **71(1)**: 44-54 (2005).

[45] Kalogirou S.A., "Solar Energy Engineering: Processes and Systems", Academic Press (2013).

[46] Hoseinzadeh S., Heyns P.S., Advanced Energy, Exergy, and Environmental (3E) Analyses and Optimization of a Coal-Fired 400 MW Thermal Power Plant, *Journal of Energy Resources Technology*, **143(8)**: 082106 (2021).